PHYSICAL REVIEW B

SOLID STATE

THIRD SERIES, VOL. 6, NO. 9 1 NOVEMBER 1972

Vibronic Effects in the Electron Paramagnetic Resonance of Mn^{++} in $Ca(OH)_2$†

F. Holuj and S. M. Quick
Department of Physics, University of Windsor, Windsor, Ontario, Canada

and

M. Rosen
Atomic Energy Commission, Beer Sheva, Israel

(Received 13 September 1971; revised manuscript received 31 May 1972)

The temperature variation of the spin-Hamiltonian parameters of Mn^{++} in $Ca(OH)_2$ single crystals was studied. The parameters b_2^0 ($=D$) and the isotropic part of the hyperfine-structure tensor A showed marked variation in the range 80–800 °K. b_2^0 showed a reversal of sign around 450 °K. The theory of orbit-lattice interaction and the theory of covalent reduction of A through spin polarization was applied to the interpretation of the temperature variance of A. The temperature variations of b_2^0 were interpreted as originating from the phonon modulations of the crystal field. The calculated values were comparable to the experimental values. Implicit temperature variations of b_2^0 were also found to be significant. Included also are the results of the velocities of sound in $Ca(OH)_2$ as functions of temperature.

I. INTRODUCTION

We present the results of investigation of the $Ca(OH)_2$: Mn^{++} system by the electron-paramagnetic-resonance (EPR) method, at temperatures which varied over the range 4.2–800 °K. This system is of interest because it presents the following problem.

The first problem is the "zero-field splitting" of the ^6S states belonging to the iron group of which Mn^{++} is a representative.[1] The theory of zero-field splitting was treated extensively by Sharma *et al.*[2–4] But these and earlier ones[5] assume rigid lattices only.

The second problem is the phonon-induced contributions to the spin-Hamiltonian parameters. This was first discussed by Walsh *et al.*[6] Subsequently, the temperature variation of the hyperfine constant for MgO: Mn^{++} was discussed by Orbach and co-workers,[1,7] and others.[8] Other cubic crystals were also investigated.[9,10] Of the remaining spin-Hamiltonian parameters only the axial parameter D in $KTiO_3$ was investigated.[11]

The ^8S-state ions of the rare-earth group present similar problems. The temperature variation of the hyperfine structure for CaF_2: Eu^{++} (and other fluorite-type hosts) has already been discussed.[12,13] Other spin-Hamiltonian parameters for $CaWO_4$: Gd^{+3} were discussed recently by Harvey and Kiefte.[14]

In addition, the host crystal $Ca(OH)_2$ itself is interesting. The absence of H bonding between OH^- ions and the hexagonal symmetry of its lattice makes it possible to set up a simple model of crystal field. Moreover, it is only recently that we have been able to obtain this material as large single crystals containing Mn^{++} impurity.

II. $Ca(OH)_2$ CRYSTALS AND EXPERIMENTAL PROCEDURE

X-ray studies have shown[15–18] that $Ca(OH)_2$ belongs to the hexagonal system, with space group $P(3, 2/m, 1)$, CdI_2 type or D_{3d}^3. A projection of the structure is shown in Fig. 1(a). Ca atoms lie in the invariant positions (0, 0, 0), with point symmetry D_{3d}. O and H atoms lie in the special positions $\pm(\frac{1}{3}, \frac{2}{3}, z_0)$ and $\pm(\frac{1}{3}, \frac{2}{3}, z_h)$, respectively, both with point symmetry $3m$. Figure 1(b) shows the unit cell. It contains one molecule. The H positions were first postulated by Bernal and Megaw.[16] They have since been confirmed by x-ray diffraction,[18] neutron diffraction,[19] and nuclear-magnetic resonance.[20]

The $Ca(OH)_2$ structure consists of two sheets of

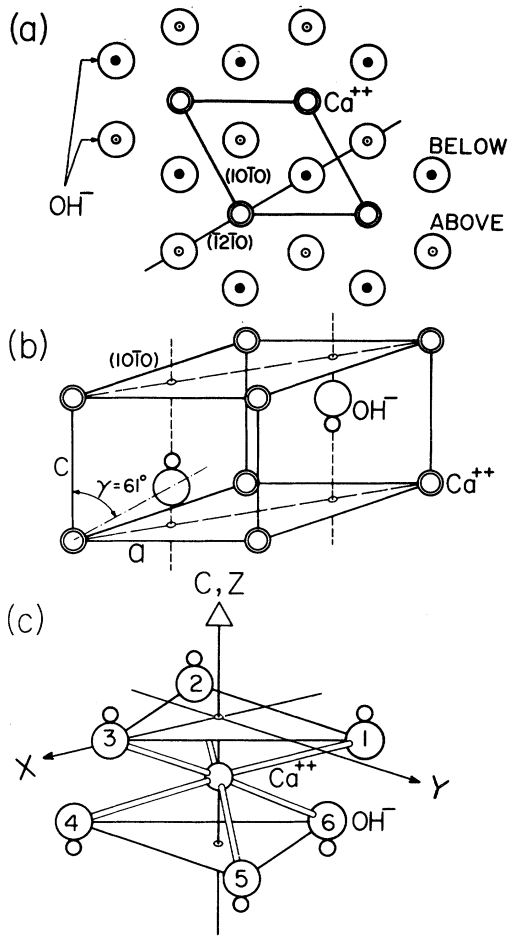

FIG. 1. $Ca(OH)_2$ crystallography. (a) Projection of the structure in the (0001) plane. The unit cell is shown in heavy outline. The threefold axis passes through the Ca^{++} sites. (b) The details of the hexagonal unit cell. (c) The geometry of the Ca^{++} site. The octahedron is slightly compressed along the c axis [or (0001) direction]. The regular octahedron has $\gamma = 54.7°$. Note the designation of planes and the crystal field axes which are mentioned in the text.

hydroxyl ions lying in the (0001) plane. A sheet of Ca ions is sandwiched between them. Each Ca ion is surrounded by six OH groups forming a slightly compressed octahedron [Fig. 1(c)]. Neutron-diffraction studies revealed that the motion of hydrogen is in the (0001) plane only.[19,21] Consequently, there are no hydrogen bonds. The crystal is very soft (2 on Moh's scale) and has a perfect cleavage along (0001).

Single crystals of $Ca(OH)_2$ were obtained by slow diffusion of NaOH and $CaCl_2$ in an aqueous solution that was free of CO_2 and O_2. They were doped with Mn^{++} during their growth.

An x-band spectrometer, utilizing a circulator and a simple detection method, was used. The phase-sensitive detector operated at 100 kHz/sec. A crystal-rotating mechanism developed earlier in this laboratory was employed for anisotropy studies at room temperature.[22] This mechanism enabled the crystal to be rotated about a horizontal axis. Using this device together with a magnet which is able to rotate about its vertical axis, any arbitrary orientation of the crystal relative to the external magnetic field could be attained. A cavity for studies in the temperature range below room temperature was of plastic, with the inner surface sputtered with gold. For the high-temperature work (300–800 °K) we used a glass cavity, which was also gold plated. Both cavities, whose loaded Q's were about 6000 and 4000, respectively, operated in the TE_{011} mode. Temperatures were measured with uncalibrated thermocouples of copper constantan (80–300 °K), and Pt/Pt-10% Rh (above 300 °K). The accuracy was estimated to be ±2 °C.

III. RESULTS

A. Qualitative Observations

Typical recordings of the spectrum taken with the applied magnetic field along the c axis are shown in Fig. 2. The linewidths as functions of temperature and the additional splittings due to the superhyperfine-structure (SHFS) interaction with hydrogen of the OH^- group are illustrated. A peculiarity of the SHFS splitting, here, is its dependence on the fine-structure (FS) component. As shown in Fig. 2, they are well resolved only for the transitions $\frac{1}{2} \leftrightarrow +\frac{3}{2}$ and $(+\frac{3}{2} \leftrightarrow +\frac{5}{2})$. This is probably due to different relaxation times.

The spectrum at all crystal orientations consisted of six groups of five lines. This indicated that there was only one Mn^{2+} ion per unit cell and that the hyperfine structure (HFS) splitting was larger than the FS splitting. The angular variation pattern of the resonances was symmetrical about the c axis. The spectrum was isotropic for rotation of $\vec{H}$ in the (0001) plane. The spectrum exhibited no symmetry at all for a rotation of $\vec{H}$ in the $(10\bar{1}0)$ plane nor in any other arbitrary plane through the c axis. This behavior is consistent with Mn^{++} substituting for calcium. The c axis is thus the magnetic z axis. This also indicates the presence of a large b_4^3 parameter.

B. Spin Hamiltonian for Room-Temperature Spectra

The room-temperature spectrum was analyzed using the spin Hamiltonian adapted for D_{3d} symmetry:

$$\mathcal{H}(S) = \mu_B \vec{H} \cdot \tilde{g} \cdot \vec{S} + \vec{I} \cdot \tilde{A} \cdot \vec{S} + \tfrac{1}{3} b_2^0 O_2^0 + \tfrac{1}{60} (b_4^0 O_4^0 + b_4^3 O_4^3). \quad (1)$$

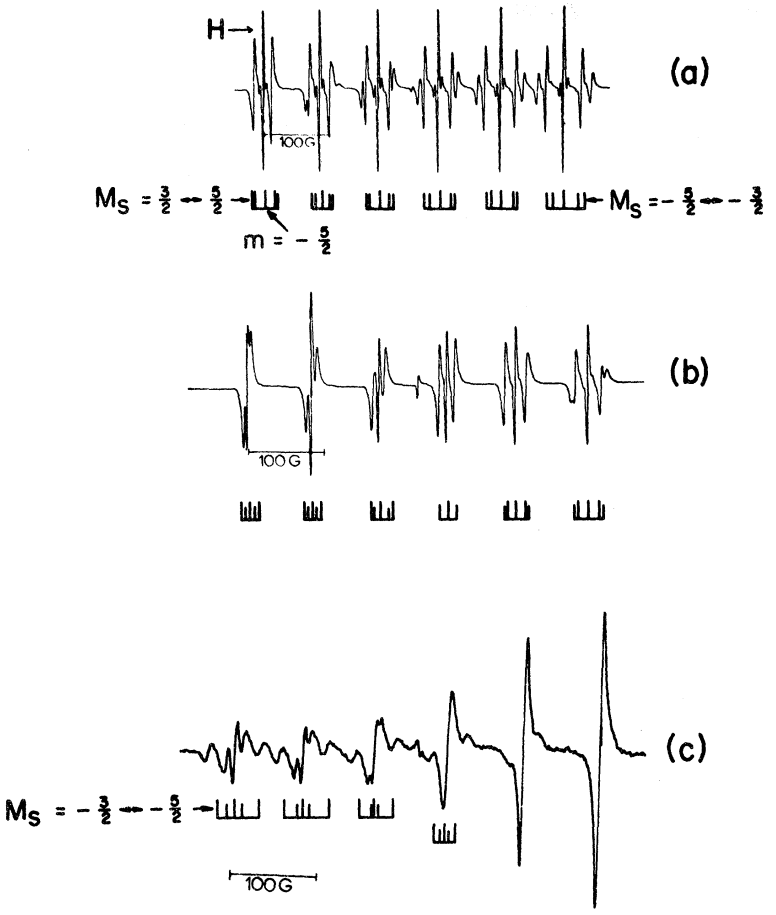

FIG. 2. Recordings of the ESR spectrum of Mn^{++} impurity in $Ca(OH)_2$ for $\vec{H}$ along the $(\bar{1}\,2\,\bar{1}\,0)$ direction (i.e., perpendicular to the c axis). We have (a) 96 °K, (b) 300 °K, and (c) 609 °K.

This spin Hamiltonian was diagonalized by a perturbation method which included second-order terms. The parameters obtained in this way were

$$g_{\parallel} = g_{\perp} = 2.0010 \pm 0.0005, \quad A_{\parallel} = -92.05,$$

$$A_{\perp} = -90.28 \pm 0.15,$$

$$b_2^0 = -6.7 \pm 0.5\ \text{G}, \quad b_4^0 = -2.48 \pm 0.5\ \text{G}, \quad b_4^3 \neq 0.$$

The sign of b_2^0 was obtained from a separate measurement at liquid-helium temperature; that of the HFS tensor components was assumed to be nagative.

C. Temperature Variations

The spectra shown in Fig. 2 indicate that as the temperature of the crystal varies from 80 to 609 °K, the FS components reverse their order. For example, the FS components of the $m = -\frac{5}{2}$ line cross over at about 300 °K, whereas those of the $m = +\frac{5}{2}$ line do so at about 609 °K. The FS components of other HFS lines cross over at temperatures between these two. This behavior indicates that b_2^0 reverses sign.

The spectrum did not undergo abrupt changes which would indicate discontinuous changes in the spin-Hamiltonian parameters. The crystal behaved reversibly at all temperatures up to about 825 °K. At this temperature and above the crystal starts to decompose.

The temperature variations were investigated in five experimental runs in which the spectrometer-cavity system was stabilized at 30 different temperatures. At each temperature the resonant fields were measured. The results were used to compute the spin-Hamiltonian parameters by the method described in Sec. IV. The results for b_2^0 and for A are presented in Fig. 3. Here A is the Fermi contact term

$$A = \tfrac{1}{3}(A_{\parallel} + 2A_{\perp}) . \tag{2}$$

The temperature variations of the g values were immeasurably small, and that of b_4^0, while showing some decrease with temperature, also showed much scatter. b_4^3 was not investigated.

IV. INTERPRETATION OF TEMPERATURE VARIATIONS

There were two spin-Hamiltonian parameters which showed much temperature variation; the

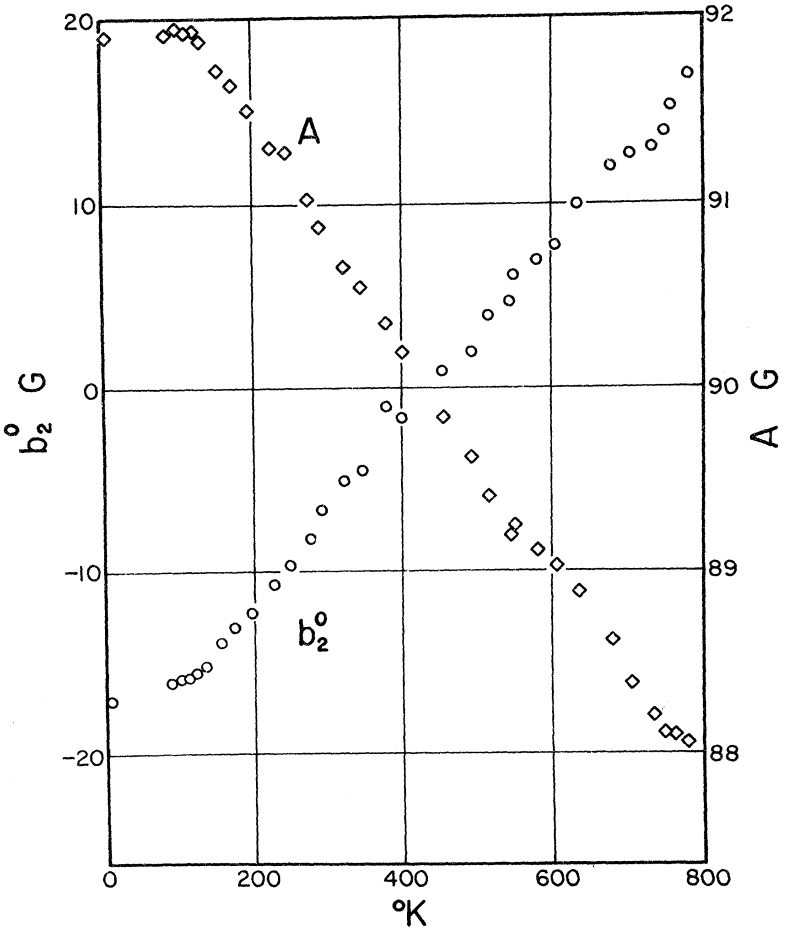

FIG. 3. Experimental temperature variations of A (the isotropic hyperfine constant of Mn^{++}, diamonds) and of b_2^0 for $Ca(OH)_2:Mn^{++}$ (open circles).

axial parameter b_2^0 (or D) and the HFS parameter A. We discuss their temperature variations in terms of the orbit-lattice interaction first and in terms of covalency last.

A. Orbit-Lattice Hamiltonian in D_{3d} Symmetry

In the presence of an electric dipole μ and a change e', the potential at a distance $(\vec{S}_i - \vec{r})$ is

$$V = \frac{\mu \cos\gamma}{|\vec{S} - \vec{r}|^2} + \frac{e'}{|\vec{S} - \vec{r}|} . \tag{3}$$

$\vec{S}_i$ is the position of the neighboring ion in a displaced position from its equilibrium position $\vec{R}_i$, $\vec{r}$ is the position vector of an electron, and γ is the angle between $\vec{R}_i$ and the c axis. The first term of Eq. (3) represents the potential due to a distant-point dipole for $\vec{R}_i \approx \vec{S}_i \gg \vec{r}$. We expand this in Legendre polynomials and the first few terms of this expansion are[23]

$$V = \sum_i \frac{e' r^l}{S_i^{l+1}} P_l(\cos\omega) + \mu \cos\gamma \left[\left(\frac{8}{3} \frac{r^2}{S_i^4} + \frac{8}{7} \frac{r^4}{S_i^6} + \cdots \right) P_2(\cos\omega) + \left(\frac{128}{35} \frac{r^4}{S_i^6} + \frac{128}{77} \frac{r^6}{S_i^8} + \cdots \right) P_4(\cos\omega) + \cdots \right] . \tag{4}$$

The orbit-lattice Hamiltonian as used in the literature[6] can be obtained systematically as follows: We expand V around $\vec{R}_i$ in a Taylor series:

$$V = V_0 + (\vec{\nabla} V)_0 \cdot \vec{\sigma}_i + \tfrac{1}{2} \vec{\sigma}_i \cdot (\vec{\nabla}^2 V)_0 \cdot \vec{\sigma}_i , \tag{5}$$

where $\vec{\sigma}_i = \vec{S}_i - \vec{R}_i$ and V_0 is the static potential. All derivatives are evaluated at equilibrium separation. The second term of Eq. (5) is the orbit-lattice interaction, which we expand (after multiplying by e),

$$V_{OL} = \{ B Y_m^* \vec{R}_i \cdot \vec{\sigma}_i + A \vec{\sigma}_i \cdot [\nabla (S_i^2 Y_m^*)]_0 \} Y_m \tfrac{4}{5} \pi r^2 , \tag{6a}$$

where Y_m stands for $Y_2^m(r)$, Y_m^* stands for $Y_2^m{}^*(\vec{S}_i)$,

$$A = (8e\mu \cos\gamma)/3R^5 + ee'/R^4 ,$$
$$B = (16e\mu \cos\gamma)/R^5 + 5ee'/R^4 . \tag{6b}$$

Since all OH^- ions are equidistant, we have set $\vec{R}_i = R\vec{r}_i$. Equation (6a) must be expanded in normal modes appropriate for XY_6 of D_{3d} symmetry.

We choose the coordinates (X, Y, Z) and number the (OH^-) groups as indicated in Fig. 1(c). e' and μ are the charge and the dipole on OH^- ions. They are both negative at the Ca^{++} site in $Ca(OH)_2$.

The result of this expansion is

$$V_{OL} = r^2 \Big[\sum_{j=1,2} V(jA_{1g}) C(A_{1g}) q(jA_{1g}) + \sum_{j=1,2} \sum_{k=1,3} V(jE_2^k) \sum_{n=1,2} C(jE_2(n)) q^*(jE_2^k(n)) \Big] . \quad (7)$$

$V(j\Gamma_i^k)$ are coefficients coupling the XY_6 cluster mode $q(j\Gamma_i^k(n))$ to electron operator $C(j\Gamma_i(n))$, where C's are defined in Table I. It should be noted here that, excepting $C(A_{1g})$, they are not operator eigenstates of energy in D_{3d} symmetry. Also, only the symmetric representations A_{1g} and E_{2g} are involved—the latter doubly degenerate $(n = 2)$. There are several q's that transform according to the same representation (in fact, two as A_{1g} and six pairs as E_{2g}). Among the five operator eigenstates (Table I), one transforms as A_{1g} and the remaining two pairs as $1E_{2g}(n)$ and $2E_{2g}(n)$. Figure 4 should serve as an aid to Eq. (7). Thus, to write down terms involving the coefficient $V(2E_2^2)$, we have

$$r^2 V(2E_2^2) [C(2E_2(1))\, q(2E_2^2(1)) + C(2E_2(2))\, q(2E_2^2(2))] ,$$

i.e., use the terms connected by lines running from right to left. The quantities (x_i, y_i, z_i) in Table I are the components of the vector $\vec{\sigma}_i - \vec{\sigma}_{i+3}$, i.e., the difference between the displacements of two diagonally opposite OH^- ions (Fig. 1).

The second-order term is

$$\tfrac{1}{2} e [\vec{\sigma}_i \cdot (\vec{\nabla}^2 V) \cdot \vec{\sigma}_i] = \Big(\frac{1}{2R} Y_m^* [F (\vec{r}_i \cdot \vec{\sigma}_i)^2 - B\sigma_i^2] - \frac{B}{R} \vec{\sigma}_i \cdot \vec{\nabla} (S_i^2 Y_m^*) (\vec{r}_i \cdot \vec{\sigma}_i) + \frac{A}{2R} [(\vec{\sigma}_i \cdot \vec{\nabla})^2 S_i^2 Y_m^*] \Big) r^2 \frac{4\pi}{5} Y_0 , \quad (8a)$$

where

$$F = (128 e\mu \cos\gamma)/R^5 + 35 ee'/R^4 . \quad (8b)$$

The summation over the index i is implied in all the above formulas.

B. Hyperfine-Structure Constant A

The basis of the theory is the admixture of the excited configurations $(3d^4ns)$ into the ground-state configuration $3d^5$ of Mn^{++}.[6,9] The existing theories use only the orbit-lattice interaction Hamiltonian of Eq. (7). To those we must add the second-order axial crystalline field[6]:

$$|3d'\rangle = |3d\rangle - \sum_n \frac{\langle ns | V_{OL} + V_{ax} | 3d \rangle}{E(3d) - E(ns)} |ns\rangle , \quad (9)$$

where V_{ax} is defined below. Since the hyperfine magnetic-field operator of the kth electron at the nucleus is

$$H_{hyp} = \tfrac{8}{3} \pi g \mu_B s_{zk} \delta(\vec{r}_k) ; \quad (10)$$

the first-order terms of H_{hyp} cancel between the states in Eq. (9), and we are left with[6]

$$\langle {}^6S' M_s | H_{hyp} | {}^6S' M_s \rangle = \frac{8\pi}{75} g\mu_B M_s \times \sum_{nn'} \frac{\langle 3d | r^2 | ns \rangle \langle n's | r^2 | 3d \rangle}{[E(3d) - E(ns)][E(3d) - E(n's)]} \langle ns | \delta(\vec{r}) | n's \rangle \times \Big(|V_{ax}|^2 + \Big| \sum_{j=1}^{2} V(jA_{1g}) q(jA_{1g}) \Big|^2 + \sum_{n=1}^{2} \Big| \sum_{j=1}^{2} \sum_{k=1}^{3} V(jE_{2g}^k) q(jE_{2g}^k(n)) \Big|^2 \Big) . \quad (11)$$

TABLE I. Orbit-lattice coupling coefficients and normal coordinates of XY_6 molecule having D_{3d} symmetry.

$C(j\Gamma_i(n))$	$V(j\Gamma_i^k)$	$q(j\Gamma_i^k(n))$	Symmetry
$(\frac{4}{5}\pi)^{1/2} Y_0 = \{\frac{1}{2}(3z^2 - r^2)\}$	$+\frac{1}{2}\sqrt{3}\, B(3\cos^2\gamma - 1) \sin\gamma + \sqrt{6}\, A \sin\gamma$	$\{x_1 + x_2 - 2x_3 - \sqrt{3}(y_1 - y_2)\}/2\sqrt{6}$	$1A_{1g}$
	$-\frac{1}{2}\sqrt{3}\, B(3\cos^2\gamma - 1) \cos\gamma + 2\sqrt{6}\, A \cos\gamma$	$\{z_1 + z_2 + z_3\}/\sqrt{6}$	$2A_{1g}$
$(\frac{4}{5}\pi)^{1/2} (Y_2 + Y_{-2})/\sqrt{2} = \{\frac{1}{2}\sqrt{3}(x^2 - y^2)\}$	$-\frac{3}{2} B \sin^3\gamma$	$\{x_1 + x_2 + 4x_3 - \sqrt{3}(y_1 - y_2)\}/\sqrt{48}$	$1E_2^1(1)$
		$+\{x_1 - x_2 - \sqrt{3}(y_1 + y_2)\}/\sqrt{16}$	$1E_2^1(2)$
$i(\frac{4}{5}\pi)^{1/2}(Y_{-2} - Y_{-2}^*)/\sqrt{2} = \{xy\sqrt{3}\}$	$-\frac{3}{2} B \sin^2\gamma \cos\gamma$	$\{z_1 + z_2 - 2z_3\}/\sqrt{12}$	$1E_2^2(1)$
		$\frac{1}{2}\{-z_1 + z_2\}$	
	$-\frac{3}{2} A \sin\gamma$	$\{x_1 + x_2 - 2x_3 + \sqrt{3}(y_1 - y_2)\}/\sqrt{24}$	$1E_2^3(1)$
		$\{\sqrt{3}(x_2 - x_1) + y_1 + y_2 - 2y_3\}/\sqrt{24}$	$1E_2^3(2)$
$(\frac{4}{5}\pi)^{1/2}(Y_{-1} + Y_{-1}^*)/\sqrt{2} = zx\sqrt{3}$	$-3B \sin^2\gamma \cos\gamma$	$= q\{1E_2^1(1)\}$	$2E_2^1(1)$
		$= -q\{1E_2^1(2)\}$	$2E_2^1(2)$
$i(\frac{4}{5}\pi)^{1/2}(Y_{-1} - Y_{-1}^*)/\sqrt{2} = zy\sqrt{3}$	$3B \sin\gamma \cos^2\gamma - 3A \sin\gamma$	$= q\{1E_2^2(1)\}$	$2E_2^2(1)$
		$= -q\{1E_2^2(2)\}$	$2E_2^2(2)$
	$3\sqrt{2}A \cos\gamma$	$\{x_1 + x_2 + x_3\}/\sqrt{6}$	$2E_2^3(1)$
		$\{y_1 + y_2 + y_3\}/\sqrt{6}$	$2E_2^3(2)$

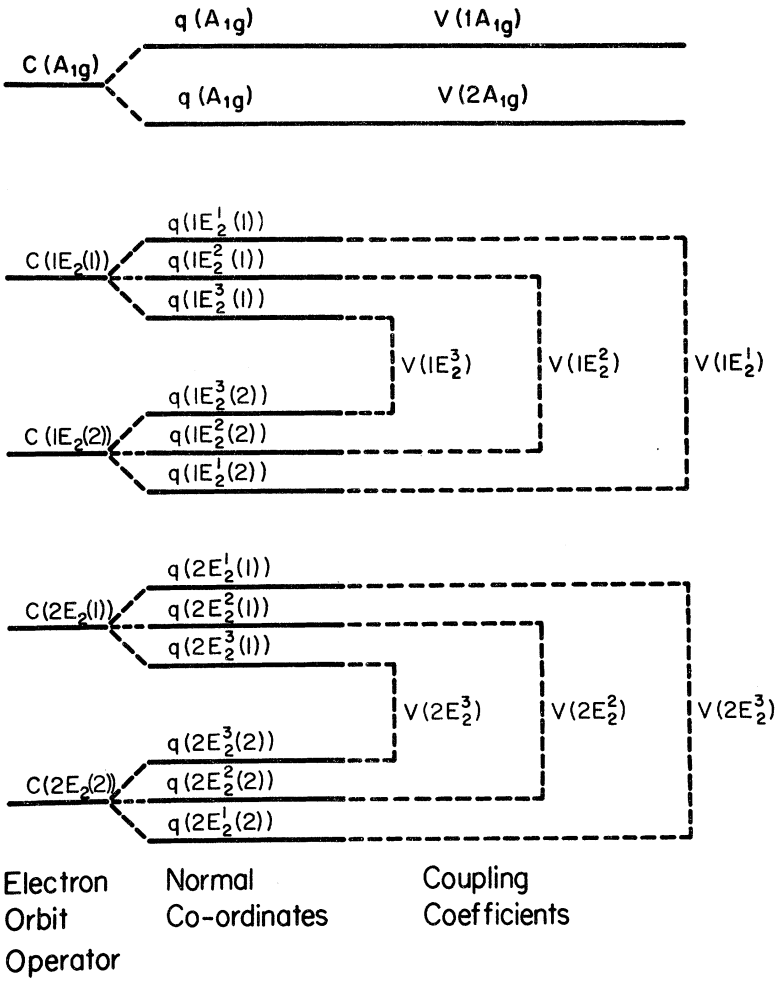

FIG. 4. Coupling scheme of normal modes $q(j\Gamma)$ of XY_6 cluster of D_{3d} symmetry to operator eigenstates transforming as representations of D_{3d} point group [see Eq. (7)].

In Eq. (11) we form products only between components having the same symmetry, e.g., cross products like $q(jE^k_{2g}(1))\, q^*(jE^k_{2g}(2))$ are zero. Also, the cross products involving V_{ax} and one of the q's contribute nothing, since V_{ax} is independent of the vibrational coordinates and its product with q averages to zero.

To adapt Eq. (11) to a form suitable for computations, we introduce the following quantities: For any product $V(m)V(n)q(m)q^*(n)(R^4/ee')^2$ in Eq. (11), we have

$$F = V'(m)\,V'(n)\left(\frac{\hbar}{k_B}\right)^2 \times \int_0^{k_D} \frac{v_t^3}{\omega_{k_\sigma}}\left(\frac{2}{e^{\hbar\omega_{k_\sigma}/k_B T}-1}+1\right)\sum\langle\alpha\beta ij\rangle_\sigma k^2\,dk\,, \tag{12}$$

where a summation over α, β, i, and j is implied and

$$V'(m) = V(m)/(N_m^{1/2} ee'/R^4)$$

and k_D depends on the model used for lattice vibrations. Also

$$\langle\alpha\beta ij\rangle_\sigma = (1/4\pi) \times \int\int \sin\Theta_k\, d\Theta_k\, d\varphi_k\, \Phi^\sigma_\alpha\, \Phi^\sigma_\beta \sin(\vec{k}\cdot\vec{R}_i)\sin(\vec{k}\cdot\vec{R}_j)\,. \tag{13}$$

Here Φ^σ_α denotes the direction cosine along the α axis of ionic displacement in longitudinal or transverse mode, and Θ_k and φ_k are the spherical polar angles of the wave vector k. Using spherical Bessel functions, the integration in Eq. (13) was done without any approximations.[9,10] $\langle\alpha\beta ij\rangle_l$ and $\langle\alpha\beta ij\rangle_t$ are related:

$$\langle\alpha\alpha ij\rangle_t = \tfrac{1}{2}(1 - \langle\alpha\alpha ij\rangle_l)\,,$$

$$\langle\alpha\beta ij\rangle_t = -\tfrac{1}{2}\langle\alpha\beta ij\rangle_l\,,$$

where $\alpha \neq \beta$. A table of relationships for $\langle\alpha\beta ij\rangle_\sigma$ in D_{3d} symmetry was constructed. It was subsequently used to evaluate the sum over i and j, which is appropriate to each product $q(n)\,q^*(m)$.

1. Acoustical Branch

If, in a standard notation, $\omega_{k\sigma} = kv_\sigma$, then

$$F^\sigma_{ac}(T) = v_t^3 V'(i) V'(j) T^2 \times\left[\frac{1}{v_\sigma^3}\int_0^{T_D/T} x_\sigma dx_\sigma \sum\langle\alpha\beta ij\rangle_\sigma \left(\frac{2}{e^{x_\sigma}-1}+1\right)\right], \tag{14}$$

where $x_\sigma = \hbar\omega_{k\sigma}/k_B T$. We have used the Debye approximation and T_D is the "reduced Debye temperature"[13] [$\Theta/\sqrt[3]{3}$ for $Ca(OH)_2$]. The zero-point contribution from this branch is

$$F^\sigma_{ac}(0) = v_t^3 T_D^2 V'(i) V'(j) (1/v_\sigma^3) \int_0^1 x_\sigma dx_\sigma \sum\langle\alpha\beta ij\rangle_\sigma, \tag{15}$$

where $x_\sigma = \hbar\omega_{k\sigma}/k_B T_D$.

2. Optical Branch

We use Einstein's approximation to calculate the contribution from an optical branch having a single frequency ω_σ independent of k:

$$F^\sigma_{op}(T) = \frac{\hbar^2 v_t^3}{\omega_\sigma k_B^2} V'(i)V'(j)\left(\frac{2}{e^{\hbar\omega_\sigma/k_B T}-1}+1\right) \times\int_0^{k_D} \sum\langle\alpha\beta ij\rangle_\sigma k^2 dk, \tag{16}$$

where $k_D = (6\pi^2 N_c/V)^{1/3}$ and N_c is the number of unit cells in a crystal of volume V. It is 1.028×10^8 cm^{-1} for $Ca(OH)_2$.

Since in a standard notation $\mu_z\langle H_{hyp}\rangle = I_z S_z A(T)$, with $\mu_z = g_n\mu_N I_z/I$, we finally obtain

$$A(T) = A_R\left[1 - a_{ax} - D\sum_\sigma (F^\sigma_{ac}(T) + \sum_{r=1}^{2} F^{\sigma,r}_{op}(t))\right], \tag{17}$$

where A_R is a "rigid-lattice" HFS constant. The remaining dimensionless parameters are

$$D = \frac{8\pi}{75}\frac{g\mu_B g_N\mu_N}{A_R I}\frac{(ee')k_B^2}{R^8\hbar\rho\pi^2 v_t^3}\sum_{nn'} U_{nn'}, \tag{18}$$

$$a_{ax} = \frac{8\pi}{75}\frac{g\mu_B g_N\mu_N}{IA_R}\left|AR(3\cos^2\gamma - 1)\right|^2 \sum_{nn'} U_{nn'}. \tag{19}$$

Since the velocity of sound in $Ca(OH)_2$ is not available in the literature, we have measured it in a separate experiment. The results are shown in Fig. 5. The measurements were carried out at 10 MHz.

The results of computations based on Eq. (17) are summarized in Table II. The computation was carried out at a Debye temperature of 249 °K as obtained from the velocities of sound at room temperature and at $\mu = 1.65D$.[24] The following comments on the values in Table II must be made. The dipolar contributions are almost of the same order of magnitude as those due to the point charge. The anisotropy of $Ca(OH)_2$ causes a longitudinal and transverse vibration to bear a complicated relationship to one another. Nevertheless, the values of $\langle\alpha\beta ij\rangle_\sigma$ were computed as if the crystal were isotropic. Optical-branch contributions were assumed at two frequencies: one (E_{2g}) at 247 cm^{-1} and another (A_{1g}) at 282 cm^{-1}. As an approximation, each was assumed to contribute two transverse and one longitudinal branch.[15] These assumptions do not influence critically the net values for A, since the contribution of the optical modes steadily drops from about 20% at low temperatures to about 6% at high temperatures. We assumed the value of 2.60×10^{14} cm erg^{-2} for the sum $\sum_{nn'} U_{nn'} = U_{44}$ in Eq. (11). It was obtained from the corrected Eq. (20) of Ref. 9. It should read $4\pi(e^2/R^3)^2 U_{44} = 2.02 \times 10^{24}$ cm^{-3}. The contribution from a_{ax} was ignored since its value is estimated to be only 3.6×10^{-4}.

The quantity D_{expt} in Table II is

$$D_{expt}(T) = [A_R - A(T)]/[\textstyle\sum_\sigma(F^\sigma_{ac} + \sum_r F^{\sigma,r}_{op})]. \tag{20}$$

According to Eqs. (17) and (18), if the above theories are correct, D_{expt} should be independent of temperature. The slight dependence of (theoretical) D on T reflects the temperature variations of v_t and R. The latter depends on T through the thermal expansion of the crystalline parameters. The subsequent decrease of D above 300 °K, however, is accidental. This was because the value of v_t at 300 °K was assumed at temperatures above this.

C. Axial Parameter

We can estimate the magnitude of vibronic contribution to the spin-Hamiltonian parameter b_2^0 as follows: Using Eq. (8a), the second-order term involving Y_0^*, only, is

$$e\sum_i \vec{\sigma}_i\cdot\vec{\nabla}^2 V\cdot\vec{\sigma}_i = \left[\left(\frac{F}{2R}(3\cos^2\gamma - 1) + \frac{2B}{R}\right)\sum_i(\vec{\sigma}_i\cdot\vec{r}_i)^2 - \left(\frac{A}{R} + \frac{B}{2R}(3\cos^2\gamma - 1)\right)\sum_i \vec{\sigma}_i^2 - \frac{6B}{R}\sum_i z_i n_i \vec{\sigma}_i\cdot\vec{r}_i + \frac{3A}{R}\sum_i z_i^2\right] r^2\left(\frac{4\pi}{5}\right)^{1/2} Y_0(\vec{r}) \equiv \sum_i \Delta_0(\vec{\sigma}_i) r^2\left(\frac{4\pi}{5}\right)^{1/2} Y_0(\vec{r}), \tag{21}$$

where (n_i, m_i, l_i) are the direction cosines of $\vec{r}_i$. Using the notation of Ref. 1, the crystalline axial Hamiltonian is

$$V_{ax} = \textstyle\sum_i (\frac{4}{5}\pi)^{1/2} B_2^0(\vec{R}_i) r^2 Y_0(\vec{r}), \tag{22}$$

where

$$B_2^0(\vec{R}_i) = (\tfrac{4}{5}\pi)^{1/2} ARY_0^*. \tag{23}$$

Neglecting the first-order terms, the axial part of Eq. (5) is

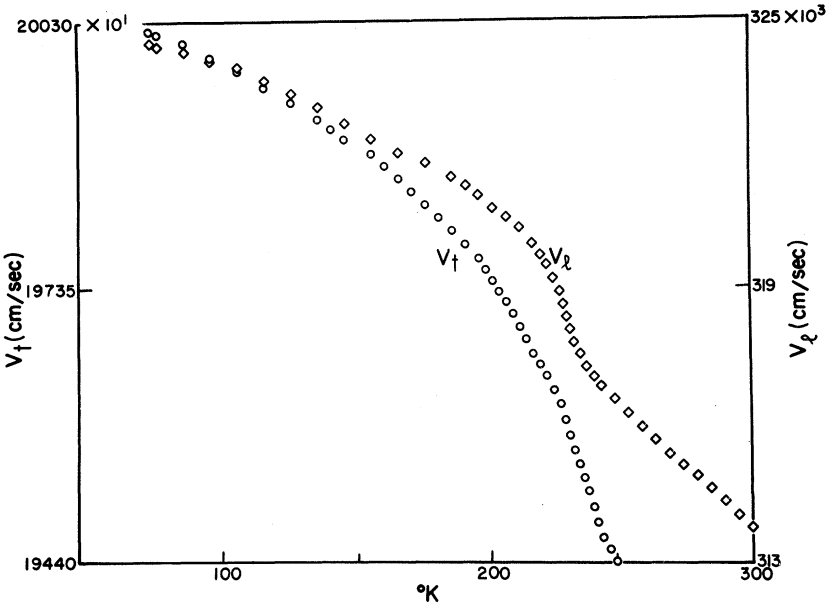

FIG. 5. Velocities of sound in $Ca(OH)_2$ as functions of temperature. The longitudinal velocity v_l is marked by diamonds and the transverse velocity v_t by open circles.

$$eV = \left(1 + \frac{\sum_i \Delta_0(\vec{\sigma}_i)}{B_2^0}\right) V_{ax} , \tag{24}$$

where

$$B_2^0 = \sum_i B_2^0(\vec{R}_i) .$$

The bracketed term in Eq. (24) should now multiply the second-order axial term of the spin Hamiltonian in Eq. (1). In terms of the spin-Hamiltonian parameter b_2^0, Eq. (24) is therefore

$$b_2^0(T) = [1 + \sum_i \Delta_0(\vec{\sigma})/B_2^0]\, b_{2R}^0 . \tag{25}$$

Next, we expand Eq. (25) in normal modes:

$$\begin{aligned}\sum_i \Delta_0(\vec{\sigma}_i)/B_2^0 = {} & W_1 [q^2(2A_{1g}) \cos^2\gamma + q^2(1A_{1g}) \sin^2\gamma \\ & - 2q(1A_{1g}) q(2A_{1g}) \sin\gamma \cos\gamma] \\ & + W_2 \sum_i \vec{\sigma}_i^2 + W_3 q^2(2A_{1g}) \\ & + W_4 q(1A_{1g}) q(2A_{1g}) ,\end{aligned} \tag{26}$$

where

$$\begin{aligned} W_1 &= (3/RB_2^0)[F(3\cos^2\gamma - 1) + 4B] , \\ W_2 &= -(1/2RB_2^0)[2A + B(3\cos^2\gamma - 1)] , \\ W_3 &= (18A - 36B)/RB_2^0 , \\ W_4 &= 36B \sin\gamma \cos\gamma / RB_2^0 . \end{aligned} \tag{27}$$

In Eq. (26), W_1 couples the "breathing" mode. W_2 does not couple a normal mode but a random displacement. W_3 and W_4 couple, respectively, a square of the z component of the breathing mode and a product of the two totally symmetric modes.

It is convenient to rewrite this and previous formulas in an expression similar to Eq. (17):

$$b_2^0(T) = [1 + D' \sum F_{ac}(T)] b_{2R}^0 , \tag{28}$$

where b_{2R}^0 is b_2^0 and is appropriate for a "rigid" lattice,

$$D' = k_B^2/(\rho\pi^2 \hbar v_t^3) , \tag{29}$$

and F_{ac} is analogous to Eq. (12) except that we replace V with appropriate W. We shall neglect optical contribution.

The results based on Eqs. (26)–(28) have been computed separately for each term of Eq. (26) and are presented in Table III. We should reject contributions of columns 2 and 3 as they give the wrong sign. The breathing mode seems to give a contribution which is not only of correct sign but also of the right order of magnitude. So does column 4. If we add columns 1 and 4, the result is in good agreement with experiment.

TABLE II. Orbit-lattice model of A in the EPR spectra of $Ca(OH)_2$: Mn^{++}. $\mu = 1.65D$ and $\Theta_D = 249$ °K.

T °K	$10^{-5}F_{ac}$	$10^{-5}F_{op}$	$10^{10}D$	$10^9 D_{expt}$	$\lvert A_R - A(T)\rvert$ (G) Theor.	Expt.
0	12.97	3.313	3.691	4.442	0.0557	0.670
100	19.09	3.505	3.691	3.201	0.07724	0.670
200	37.93	4.504	3.770	2.906	0.1482	1.142
300	60.33	5.727	3.918	2.945	0.2397	1.802
400	84.78	7.306	3.870	2.837	0.3301	2.42
500	111.6	8.995	3.822	2.744	0.4269	3.065
600	140.8	10.12	3.766	2.626	0.5296	3.684
700	172.4	12.31	3.729	2.431	0.6378	4.157
800	206.1	14.02	3.683	2.247	0.7511	4.582

TABLE III. Orbit-lattice model of b_2^0 in the EPR spectrum of Ca(OH) : Mn^{++}, $\mu = 1.65$ and $\Theta_D = 249$ °K. Numbering of contributions follows that in Eqs. (26) and (27).

T	$10^{-21} F_{ac}$ (°K^{-2})					$(b_{2R}^0 - b_2^0(T))$				
°K	1	2	3	4	$10^{22}D$ (°K)	1	2	3	4	Expt.
0	−0.803	0.127	5.323	−0.225	1.022	−1.765	0.279	11.70	−0.494	−4.5
100	−1.517	0.243	10.25	−0.497	1.022	−3.334	0.535	22.53	−1.092	−5.61
200	−2.853	0.466	19.09	−0.929	1.057	−6.484	1.06	43.39	−2.112	−9.28
300	−4.349	0.720	28.66	−1.35	1.112	−10.40	1.722	68.53	−3.228	−15.50
400	−5.859	0.9873	38.23	−1.804	1.112	−14.01	2.361	91.39	−4.314	−19.90
500	−7.426	1.272	47.95	−2.264	1.112	−17.76	3.042	114.7	−5.414	−24.20
600	−9.047	1.574	57.83	−2.732	1.112	−21.63	3.765	138.3	−6.532	−23.1
700	−10.72	1.895	67.86	−3.205	1.112	−25.64	4.531	162.3	−7.663	−34.00
800	−12.45	2.233	78.02	−3.685	1.112	−29.78	5.340	186.6	−8.812	−40.30

D. Covalency Effect

We limit this discussion to the role covalency plays in the dependence of A on temperature. Simanek and Huang[25] obtained the values of the coefficient C of Ref. 6 that was only 50% lower than the corresponding experimental C for the MgO : Mn^{++} system. Lue and Huang[26] also treated the Mn^{++} impurity in MgO and other crystals, but they did not include the spin-exchange effects which seems to dominate the covalent reduction of the hyperfine constant in Mn^{++}.[27] Consequently we shall base our discussion on Ref. 25.

To this purpose we express the operators C in Table I, so that they transform as the two bases of E_{2g} representation of D_{3d} point group and which form the σ bonds with OH^-. For crystal fields of reasonable magnitude one result is

$$\begin{aligned} \varphi_v &= a^c |XY\rangle - a^s |ZY\rangle , \\ \varphi_u &= a^c |X^2 - Y^2\rangle + a^s |ZX\rangle , \end{aligned} \tag{30}$$

where for a Ca^{++} site in $Ca(OH)_2$, one set of values of a^s and a^c is 0.7463 and 0.6657, respectively.

The antibonding molecular σ orbitals formed from φ_i and an appropriate linear combination of the ligand orbitals χ_i is

$$\psi_i = N(\varphi_i - \lambda_\sigma \chi_i) . \tag{31}$$

Now, while ψ_i is orthonormal to the s-type orbitals of Mn^{++}, φ_{ns}, the vibrational distortions of the complex $Mn(OH)_6$, destroys this. The resultant ψ_i' now have finite overlaps with φ_{ns}. Simanek and Huang[25] calculated these overlaps as functions of bond length through the relation

$$\langle \psi_i' | \varphi_{ns} \rangle = \left(\lambda_\sigma \frac{\partial S_{ns}}{\partial R} + S_{ns} \frac{\partial \lambda_\sigma}{\partial R} \right) Q_i , \tag{32}$$

where Q_i is a normal coordinate having the same symmetry as ψ_i and $S_{ns} = \langle 2p_\sigma | \varphi_{ns} \rangle$. There are several vibrational modes which couple to the ψ_i states, but two of them are particularly important:

$$Q_v = q(1E_2^2(2)) \cos\gamma - q(1E_2^1(2)) \sin\gamma ,$$

$$Q_u = q(1E_2^2(1)) \cos\gamma - q(1E_2^1(1)) \sin\gamma . \tag{33}$$

They are the trigonal analogues of the cubic normal modes bearing the same subscript.

We orthonormalize ψ_i' and φ_{ns} by the Schmidt process and obtain

$$\psi_i'' = N(\psi_i' - \sum_{n=1}^{4} \langle \psi_i' | \varphi_{ns} \rangle \varphi_{ns}) . \tag{34}$$

We exclude from Eq. 34 the terms φ_{4s} originating from the orbit-lattice interaction as discussed previously in Sec. IV B.

The hyperfine field analogous to Eq. (11) is

$$\begin{aligned} \langle H_{hyp} \rangle &= \frac{8\pi}{3} g\mu_B s_z (\langle \psi_u'' | \delta(r) | \psi_u'' \rangle + \langle \psi_\sigma'' | \delta(r) | \psi_v'' \rangle) \\ &= \frac{8\pi}{3} g\mu_B \frac{1}{2R^2} \sum_{nn'} a_{ns} a_{n's} \langle \varphi_{n's} | \delta r | \varphi_{ns} \rangle (Q_v^2 + Q_u^2) , \end{aligned} \tag{35}$$

where we used the notation of Ref. 25. The correction to A for the covalency effect (in G) is

$$\Delta A_{cov} = -D_{cov} \sum_\sigma [F_{ac,cov}^\sigma(T) + F_{op,cov}^\sigma(T)] , \tag{36}$$

where

$$\begin{aligned} D_{cov} &= \frac{8\pi}{3} \frac{g_N \mu_N}{I} \frac{k_B^2}{R^2 \rho \pi^2 \hbar v_t^3} \sum_{nn'} C_{nn'} , \\ \sum_{nn'} C_{nn'} &= \sum_{nn} a_{ns} a_{n's} \langle \phi_{n's} | \delta r | \phi_{ns} \rangle , \\ F_{ac,cov}^\sigma &= (\hbar^2/k_B^2) I . \end{aligned}$$

I stands for the integral in Eq. (12). Table IV summarizes the results of computation based on Eq. (36) and the estimated value of $\sum_{nn'} C_{nn'}$ as 1.56×10^{24} cm^{-3}. The results for ΔA, as expected are only about three times smaller than the experimental ones.

The assumptions used in obtaining the above result must be stressed: We used the values of $C_{nn'}$ for MgO crystal. Appropriate values for $Ca(OH)_2$ are expected to be similar, since the bond lengths are comparable [2.1 Å for MgO and 2.37 Å for $Ca(OH)_2$] and the covalent reduction factors for A are also similar.

TABLE IV. Covalent model of A in the EPR spectra of $Ca(OH)_2 : Mn^{++}$ $\Theta_D = 249$ °K.

T °K	$10^{-4}F_{ac,cov}$	$10^{-4}F_{op,cov}$	$10^{9}D_{cov}$	ΔA_{cov} (G)
0	0.645	1.844	1.808	0.139
100	1.060	1.952	1.808	0.210
200	2.037	2.511	1.864	0.395
300	3.153	3.194	1.955	0.629
400	4.317	4.074	1.949	0.853
500	5.551	4.986	1.943	1.089
600	6.853	5.917	1.937	1.336
700	8.221	6.858	1.930	1.593
800	9.654	7.807	1.925	1.860

V. DISCUSSION

The temperature dependence of any observable G can be divided into two parts: implicit or that due to a thermal expansion $(\partial G/\partial V)_T$ and explicit or that due to lattice vibrations $(\partial G/\partial T)_V$. The latter has been dealt with in Sec. IV. The contribution of the former is best estimated experimentally by measuring the changes of G as a function of pressure $(\partial G/\partial V)_T$ and then using the relation

$$\left(\frac{\partial G}{\partial V}\right)_T = \left(\frac{\partial G}{\partial P}\right)_T \left(\frac{\partial P}{\partial V}\right)_T . \tag{37}$$

The following trends have been confirmed for Mn^{++} in II–VI crystals: (i) Cubic spin-Hamiltonian parameters b_4^m show no implicit, or, for that matter, little temperature dependence. (ii) HFS constant A, while showing marked temperature dependence, has no implicit part. (iii) Orthorhombic parameters b_2^0 and b_2^2 have not been studied in these crystals.

Points (i) and (ii) have been confirmed for $Ca(OH)_2$. Incidentally, (i) can possibly be explained by the following argument. In expanding $V(r)$ in Taylor series [Eq. (5)], we could just as well take the derivatives with respect to the electron coordinates, as was done, for example, by Stevens.[28] Confining our remarks to b_4^0, this means that the explicit contribution to b_4^0 can only come from terms in $Y_6^m(r)$, which as is well known, do not occur in Mn^{++}.

It is very difficult to make any measurements involving pressure on $Ca(OH)_2$. This is because the crystals have a layered structure and easily disintegrate. However, expressions for b_n^m as functions of the interionic distances are available and their implicit parts can, therefore, be estimated theoretically. We limit this discussion to b_2^0. According to Sharma *et al.*,[3] the rigid lattice b_{2R}^0, can be written (in cm^{-1})

$$b_{2R}^0 = -0.07305\, B_2^0 + 2.1044(B_2^0)^2 - 1.7417(B_2^0)^2 + 4.3404 B_4^{0\prime} . \tag{38}$$

These terms are due to, respectively, spin-spin (D_{SS}), Orbach–Das–Sharma (D_{ODS}), Watanabe (D_{WC}) and Blume–Orbach (D_{BO}), mechanisms. B_2^0 is defined in Eq. (23) and $(B_4^0)'$ for D_{3d} symmetry is

$$B_4^{0\prime} = B_4^0 - \sqrt{7}/10 B_4^3 , \tag{39}$$

where using Eq. (4),

$$B_4^0 = \frac{1}{4}\sum_j \left(\frac{ee'}{R_j^5} + \frac{128}{35}\frac{e\mu\cos\gamma_j}{R_j^6} \right) \times (35\cos^4\gamma_j - 30\cos^2\gamma_j + 3), \tag{40}$$

$$B_4^3 = \frac{\sqrt{35}}{2}\sum_j \left(\frac{ee'}{R_j^5} + \frac{128}{35}\frac{e\mu\cos\gamma_j}{R_j^6} \right) \times (\cos\gamma_j \sin^3\gamma_j \cos 3\Phi_j).$$

Using thermal-expansion data for $Ca(OH)_2$, the results based on calculations based on Eq. (38) are presented in Table V. These results should be compared with the values of b_2^0 obtained experimentally. The implicit temperature variation of b_2^0 is therefore significant. Also of significance is the agreement between the signs of the calculated and experimental b_2^0 at low temperatures.

VI. SUMMARY

This paper has presented the results of the investigation of $Ca(OH)_2 : Mn^{++}$ by an EPR method at temperatures ranging from 4.2 to about 800 °K. The EPR spectrum was found to be axial at all temperatures and was consistent with Mn^{++} replacing Ca^{++}. The isotropic parameter A of the HFS and the second-order axial parameter b_2^0 for $(Ca(OH)_2$ were investigated over the temperature range 4.2–800 °K. A was found to decrease from 91.9 to 88.0 G. in this range, b_2^0 on the other hand, increased from -16.0 to $+17$ G.

Temperature variations of both parameters were discussed, in the case of A, in terms of vibronic interaction and spin polarization of ns-shell electrons by exchange potential, and in the case of b_2^0, in terms of crystal field modulation by lattice vibrations. The model included a point charge and a point dipole of XY_6 cluster in D_{3d} symmetry. Vibrational motion was handled using the spherical Bessel functions.[9] The vibronic-interaction model

TABLE V. Values of b_2^0 obtained from Eq. (30). Third nearest neighbors were included. $\mu = 1.65D$. All values are in G. The value of 22 G was obtained by extrapolation in Fig. 3.

Temperature (°K)	0	300	600	900
$D_{SS} + D_{ODS} + D_{WC}$	2.85	3.25	3.64	4.03
$+ D_{BO}$	−80.41	−75.33	−70.4	−65.68
Expt.	−21.5	−7.5	+7.7	(+22)

accounted for less than 10% of experimental values and the spin-polarization model for additional 30% in the case of A (see Tables II and IV). The lattice vibration model accounted for almost 80% of the temperature variations of b_2^0.

The implicit temperature variations of b_2^0 were also estimated using the theories proposed by Orbach *et al.*[1-3] These were found to be significant.

ACKNOWLEDGMENT

One of the authors (F. H.) wishes to acknowledge very helpful correspondence with Dr. T. J. Menne.

†Research supported by the National Research Council of Canada.

[1]E. Simanek and R. Orbach, Phys. Rev. 145, 191 (1966); R. Orbach and E. Simanek, *ibid.* 156, 383 (1967).

[2]R. R. Sharma, T. P. Das, and R. Orbach, Phys. Rev. 149, 257 (1966).

[3]R. R. Sharma, T. P. Das, and R. Orbach, Phys. Rev. 155, 338 (1967).

[4]R. R. Sharma, T. P. Das, and R. Orbach, Phys. Rev. 171, 378 (1968).

[5]M. H. L. Pryce, Phys. Rev. 80, 1107 (1950); H. Watanabe, Progr. Theoret. Phys. (Kyoto) 18, 405 (1957); M. Blume and R. Orbach, Phys. Rev. 127, 1587 (1962).

[6]W. M. Walsh, Jr., J. Jeener, and N. Bloembergen, Phys. Rev. 139, A1338 (1965).

[7]R. Calvo and R. Orbach, Phys. Rev. 164, 284 (1967).

[8]J.-T. Lue and C.-Y. Huang, Chinese J. Phys. 7, 53 (1963).

[9]T. J. Menne, Phys. Rev. B 1, 4496 (1970).

[10]C. Y. Huang and J. T. Lue, Progr. Theoret. Phys. (Kyoto) 43, 10 (1970).

[11]D. M. Mannon, Phys. Rev. B 3, 2151 (1971).

[12]T. J. Menne, D. P. Ames, and Sook Lee, Phys. Rev. 169, 333 (1968).

[13]T. J. Menne, Phys. Rev. 180, 350 (1969).

[14]J. S. M. Harvey and M. Kiefte, Can. J. Phys. 49, 995 (1971).

[15]Early references are quoted by R. W. G. Wyckoff, *The Structure of Crystals* (Reinhold, New York, 1931). Also, S. S. Mitra, in *Solid State Physics*, edited by F. Seitz and D. Turnbull (Academic, New York, 1963), Vol. 13, p. 1.

[16]J. D. Bernal and H. D. Megaw, Proc. Roy. Soc. (London) A151, 384 (1935).

[17]C. W. Bunn, L. M. Clark, and J. L. Clifford, Proc. Roy. Soc. (London) A151, 141 (1935).

[18]H. E. Petch, Phys. Rev. 99, 1635 (1955); Can. J. Phys. 35, 983 (1957); Acta Cryst. 14, 950 (1961).

[19]W. R. Busing and H. A. Levy, J. Chem. Phys. 26, 563 (1957).

[20]D. M. Henderson and H. S. Gutowsky, Am. Mineralogist 47, 1231 (1962).

[21]I. Pelah, K. Krebs, and Y. Imry, J. Chem. Phys. 43, 1864 (1965).

[22]F. Holuj, Can. J. Phys. 46, 287 (1968).

[23]W. E. Baylis, J. Chem. Phys. 51, 2665 (1969).

[24]R. T. Meyer and R. M. Meyers, J. Chem. Phys. 34, 1074 (1961).

[25]E. Simanek and N. L. Huang, Phys. Rev. Letters 17, 699 (1966).

[26]J.-T. Lue and C.-Y. Huang, Chinese J. Phys. 7, 53 (1969).

[27]E. Simanek and K. L. Muller, J. Phys. Chem. Solids 31, 1027 (1970).

[28]K. W. H. Stevens, Rept. Progr. Phys. XXX, 189 (1967).